Journal of Alloys and Compounds 509S (2011) S770–S774

Contents lists available at ScienceDirect

Journal of Alloys and Compounds

journal homepage: www.elsevier.com/locate/jallcom

Chemical surface modification for the improvement of the hydrogenation kinetics and poisoning resistance of TiFe

M. Williams [a], M.V. Lototsky [a,*], M.W. Davids [a], V. Linkov [a], V.A. Yartys [b,c], J.K. Solberg [c]

[a] South African Institute for Advanced Materials Chemistry, Department of Chemistry, University of the Western Cape, Private Bag X17, Bellville, 7535, South Africa
[b] Institute for Energy Technology, POB 40, Kjeller N-2027, Norway
[c] Norwegian University of Science and Technology, NO-7491 Trondheim, Norway

ARTICLE INFO

Article history:
Received 15 August 2010
Received in revised form 4 November 2010
Accepted 10 November 2010
Available online 18 November 2010

Keywords:
Metal hydrides
Surfaces and interfaces
Sintering
Chemical synthesis
Gas–solid reactions
Catalysis

ABSTRACT

Hydrogen storage performance of the TiFe-based materials suffers from difficulties with hydrogenation and sensitivity towards impurities in hydrogen gas reducing hydrogen uptake rates and decreasing the cycle stability. In present work the surface modification of the sintered $Ti_{1.1}Fe_{0.9}O_x$ and arc-melted TiFe was performed using autocatalytic deposition of the Pd-based catalytic layers in order to achieve improvement of the H storage characteristics. Pd deposition proved to be efficient in significant facilitation of the hydrogenation ability of the materials at moderate H_2 pressures and room temperature, even after their long exposure to air. Activation performance of the sintered $Ti_{1.1}Fe_{0.9}O_x$ is superior than that for the arc-melted TiFe. This effect was associated with the presence of the oxygen-containing suboxide $Ti_4Fe_2O_{1-x}$ in the sintered sample acting as a hydrogen transfer catalyst. γ-Aminopropyltriethoxysilane pre-functionalization and subsequent Pd–P autocatalytic deposition onto the sintered $Ti_{1.1}Fe_{0.9}O_x$ intermetallic substrate resulted in a better hydrogenation kinetics compared to the samples prepared by the conventional Pd deposition.

1. Introduction

Recently experienced difficulties in achieving uninterrupted supply of the Rare Earth metals and alloys, put a demand to develop solid hydrogen storage materials alternative to the commonly used AB_5 type alloys. Such alternatives first of all are within the alloys of Ti, Zr and Mg.

TiFe intermetallic compound is a well-studied hydrogen storage material known for more than 30 years [1]. Its reasonable storage capacity (up to 1.9 wt.% H), low pyrophoricity, abundance and low cost [2] cause interest to its applications. Improvements of the hydrogen storage performance of TiFe, including simplification of its activation and modification of the thermodynamic behaviours, can be achieved by a partial substitution of Fe with other metals, first of all, by Mn and V [2–5]. Different techniques used in the preparation of TiFe and its derivatives include smelting of the constituent elements [2,6], mechanical alloying of (Ti + Fe) or (TiH_2 + Fe), followed if necessary by annealing [7–9] or sintering of (Ti + Fe) in hydrogen atmosphere [10–12]. Despite the listed methods proved to be easily upscalable, however, special precautions must be taken during the synthesis because of the ability of the TiFe-based materials to easily pick-up oxygen, and the possibility of the formation of $TiFe_2$ which does not absorb hydrogen under acceptable pressure–temperature conditions. To avoid these complications, Ti is taken in 10–30% excess as compared to the stoichiometric Ti:Fe ratio, and/or deoxidisers like rare-earth metals are introduced. These modifications improve hydrogen storage performance, in particular two hydrogen absorption–desorption plateaux for $Ti_{1+x}Fe$ are merged thus providing high hydrogen storage capacities at reasonable hydrogen pressures [1,2,6], as well as having a benefit of an easier activation of the $Ti_{1+x}Fe$/RE alloys [13,14]. Alternatively, the activation can be facilitated by the introduction of oxygen, to yield $Ti_{1+x}FeO_y$ ($x = 0.22–0.24$, $y = 0.007–0.04$) [6].

The main drawback of TiFe and its derivatives is in their poor activation performances and low poisoning tolerance resulting in the suppression of hydrogen absorption even by trace amounts of added to hydrogen active gases like oxygen and water vapour [15,16]. Attempts to address these problems included ball milling of the parent alloy together with additives of H_2 dissociation catalysts, Pd [17] and Ni [18]. Studies of the thin films TiFe + Pd showed that Pd coating (20 nm) of TiFe (100–200 nm thick films deposited on silicon) promotes the hydrogenation of TiFe; the rate of hydrogen uptake can be further increased by annealing of the Pd-capped TiFe in air [19]. Most probably, the reason for that is in the formation of oxygen-containing phases ($Ti_4Fe_2O_{1-x}$) which were shown to easy absorb hydrogen at mild conditions [20–22]. The formation of such phases was also observed in the course of arc-melting of titanium, iron and iron oxide [6], or sintering of Ti and Fe powders in non-purified hydrogen (99.8% H_2 + 0.2% O_2), to yield TiFe as a major product [10].

* Corresponding author. Tel.: +27 21 959 9314; fax: +27 21 959 9314.
E-mail address: mlototskyy@uwc.ac.za (M.V. Lototsky).

0925-8388/$ – see front matter © 2010 Elsevier B.V. All rights reserved.
doi:10.1016/j.jallcom.2010.11.063

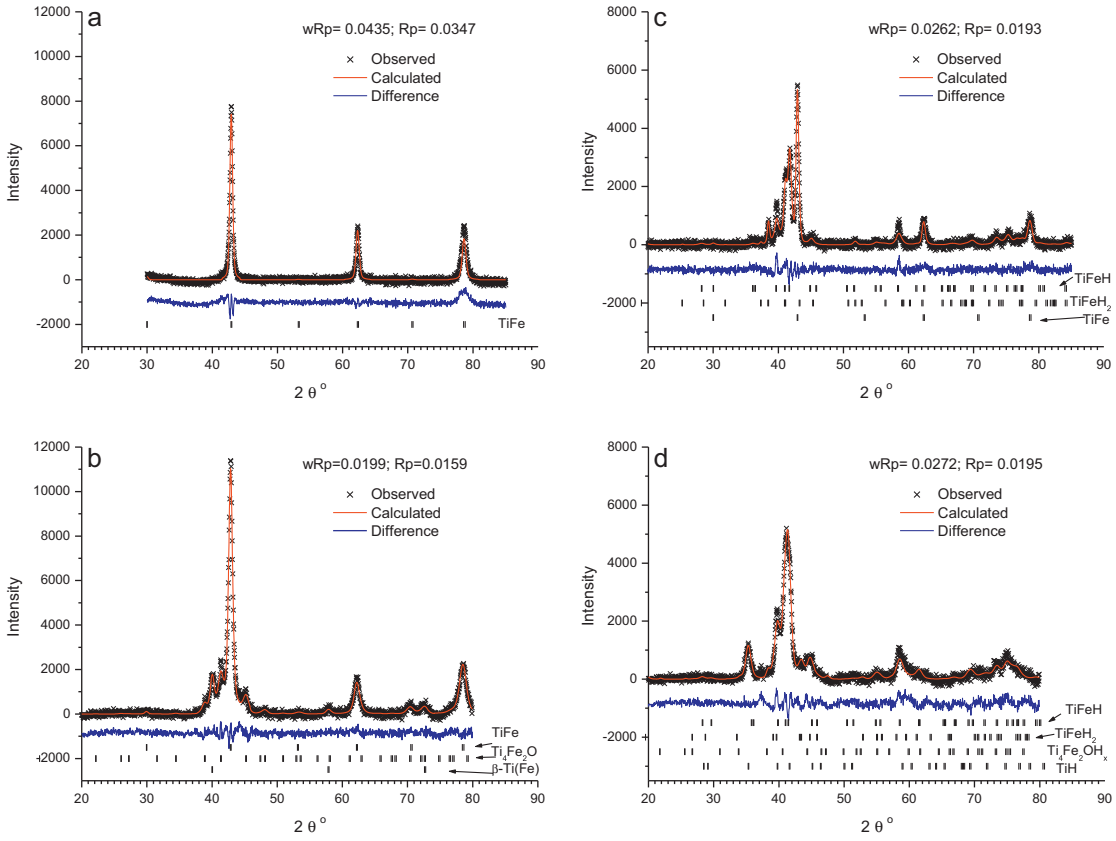

Fig. 1. XRD pattern of TiFe substrates: a – arc-melted TiFe; b – sintered $Ti_{1.1}Fe_{0.9}O_x$; c – arc-melted TiFe after hydrogenation; d – sintered $Ti_{1.1}Fe_{0.9}O_x$ after hydrogenation.

The improvement of activation and H sorption properties in the modified Ti-based intermetallides, which are very sensitive towards surface poisoning, will be more pronounced than in the case of easier activated AB_5-type materials [23]. Thus, TiFe-based substrates are very relevant in studying the effects of their surface modification. Taking into account the mentioned above sensitivity of the activation performances of TiFe to the preparation routes, it would be also important to reveal the effects of the surface modification of the TiFe substrates prepared by different methods.

This work presents experimental results on morphological and hydrogen charging characteristics of the arc-melted and sintered oxygen-containing TiFe alloy, both were surface-modified through the autocatalytic deposition of Pd(P) [24–26]. The primary objective was in the development of the Rare Earth–free hydrogen storage materials with improved activation performance and increased poisoning tolerance.

2. Experimental

TiFe intermetallide was prepared by arc-melting (Institute for Energy Technology) of the high-purity metals (>99.99%) taken in equiatomic amounts (total mass ~5.0 g) on a water-cooled copper crucible in protective argon atmosphere. Subsequently, the prepared metal ingots were pulverised by ball-milling in argon for 10 min.

Sintered $Ti_{1.1}Fe_{0.9}O_x$ was prepared by mixing Ti and Fe powders (Alfa Aesar, purity 99.99%, particle size 44 μm) in 1.1: 0.9 atomic ratio, through grinding in a mortar, and placing the mixture (~10 g) into a quartz or tungsten sample holders positioned in a quartz tube inside a tubular furnace (South African Institute for Advanced Materials Chemistry). The tube was flushed at room temperature with Ar (Afrox Ltd., 99.999%, O_2 and H_2O impurities below 10 ppm) for 1 h to displace air. This was followed by heating to 1000 °C, maintaining the high temperature for 1.0 h, and cooling down to room temperature under Ar flow.

The excess of Ti (~22% as to the stoichiometric amount in the sintered material) was chosen to (i) avoid a formation of inactive in hydrogenation $TiFe_2$ and (ii) increase the Ti/Fe ratio to allow formation of $Ti_4Fe_2O_x$. From experiments (see next section, Fig. 1, Table 1) we have found that chosen content of Ti and sintering conditions yielded a mixture of two hydride-forming constituents, TiFe and $Ti_4Fe_2O_{1-x}$ formed in ratio of approximately 3:1.

Surface modification of the TiFe-based substrate was achieved by autocatalytic deposition of palladium in hypophosphite-based baths. The materials were initially sensitized-activated in a $SnCl_2$–$PdCl_2$ colloidal solution (30 min; 300 rpm; 20 °C) prepared by dissolving 0.3 g $PdCl_2$ in 2.15 g HCl and mixing with 25 g $SnCl_2$ $2H_2O$ dissolved in 14.45 g HCl and 8.75 g KCl dissolved in 80 mL HCl. The activated powders were then accelerated in a 10% (w/v) solution of disodium ethylene-diamine-tetra-acetic acid (Na_2EDTA) for 10 min. The materials were further plated (pH ~9.0; 50 °C; 30 min; 300 rpm) in an ammoniacal bath solution, which was constituted as follows: 1.0 g L^{-1} $PdCl_2$; 27 g L^{-1} NH_4Cl; 160 mL L^{-1} NH_4OH; 4.0 mL L^{-1} HCl; 10 g L^{-1} NaH_2PO_2. A customized autocatalytic deposition technique allowing to use dilute (< 1.0 g/L) solutions of Pd salts with 100% utilization of Pd [25] was also utilized in the surface modification of the sintered $Ti_{1.1}Fe_{0.9}O_x$ based on the detection of oxygen. The technique involved surface pre-functionalization of the sintered substrate using 1.0 vol.% solutions of γ-aminopropyltriethoxysilane (γ-APTES) to facilitate the surface immobilization of Pd nuclei in the sensitization-activation process, resulting in increased densities of deposited Pd(P) particles and surface Pd loading on the intermetallide compared to that prepared without the pre-functionalization step [26].

The samples were characterised by XRD (Bruker AXS D8 Advance, Cu-Kα, $\lambda_1 = 1.5406$ Å, $\lambda_2 = 1.5444$ Å, $\lambda_2/\lambda_1 = 0.5$, $2\theta = 20–85°$), SEM (Zeiss Ultra 55, Norwegian University of Science and Technology, 4.0 kV, secondary electrons), and volumetric measurements of hydrogen absorption kinetics ($T = 20$ °C, $P_0 \sim 30$ bar H_2, for 24 h). Before the measurements of hydrogen absorption, the system was evacuated to not less than 1.0×10^{-3} mbar at room temperature/$T = 400$ °C, for 1 h.

All materials were allowed exposure to air (no less than two weeks) prior to the experimental studies of their hydrogen absorption performances.

3. Results and discussions

Summary of the obtained data on the phase-structural composition of the samples is presented in Table 1 and is given together with relevant reference information on the constituent phases [20,22,27–31]. The XRD pattern of the initial alloys and their corre-

Table 1
Phase composition of TiFe substrates[a].

	Arc-melted TiFe	Sintered $Ti_{1.1}Fe_{0.9}O_x$
Non-hydrogenated	TiFe: a = 2.9803(1) Å	TiFe: 64 wt.%; a = 2.9848(1) Å $Ti_4Fe_2O_{1-x}$: 25(3) wt.%; a = 11.350(3) Å β-Ti(Fe): 11(2) wt.%; a = 3.1878(8) Å
Hydrogenated (30 bar H_2, RT)	TiFeH: 59 wt.%; a = 2.9776(9) Å, b = 4.545(1) Å, c = 4.404(2) Å $TiFeH_2$: 15(4) wt.% a = 7.059(6) Å, b = 6.262(4) Å, c = 2.811(1) Å TiFe: 26(2) wt.%; a = 2.9797(1) Å	TiFeH: 62 wt.%; a = 3.0146(9) Å, b = 4.525(2) Å, c = 4.402(1) Å $TiFeH_2$: 15(5) wt.%; a = 6.675(9) Å, b = 6.218(9) Å, c = 2.671(4) Å $Ti_4Fe_2O_{1-x}H_y$: 7(2) wt.%; a = 11.558(6) Å TiH: 16(3) wt.%; a = 4.339(3) Å, c = 4.534(6) Å

[a]Reference data—TiFe: Space group $Pm\bar{3}m$ (221); a = 2.976 Å [27], TiFeH: Space group $P222_1$ (17); a = 2.966 Å, b = 4.522 Å, c = 4.370 Å [28], $TiFeH_2$: Space group $Cmmm$ (65); a = 7.029 Å, b = 6.233 Å, c = 2.835 Å [29], $Ti_4Fe_2O_{1-x}$: Space group $Fd\bar{3}m$ (227); a = 11.33. . .11.35 Å (x = 0. . .0.75) [20,22], $Ti_4Fe_2O_{1-x}H_y$: Space group $Fd\bar{3}m$ (227); a = 11.4. . .11.9 Å (x = 0.4, y = 1.3. . .5.6) [20], β-Ti(Fe): Space group $Im\bar{3}m$ (229); a = 3.14 Å ($Ti_{0.75}Fe_{0.25}$) [30], TiH: Space group $P4_2/n$ (86); a = 4.21 Å, c = 4.60 Å [31].

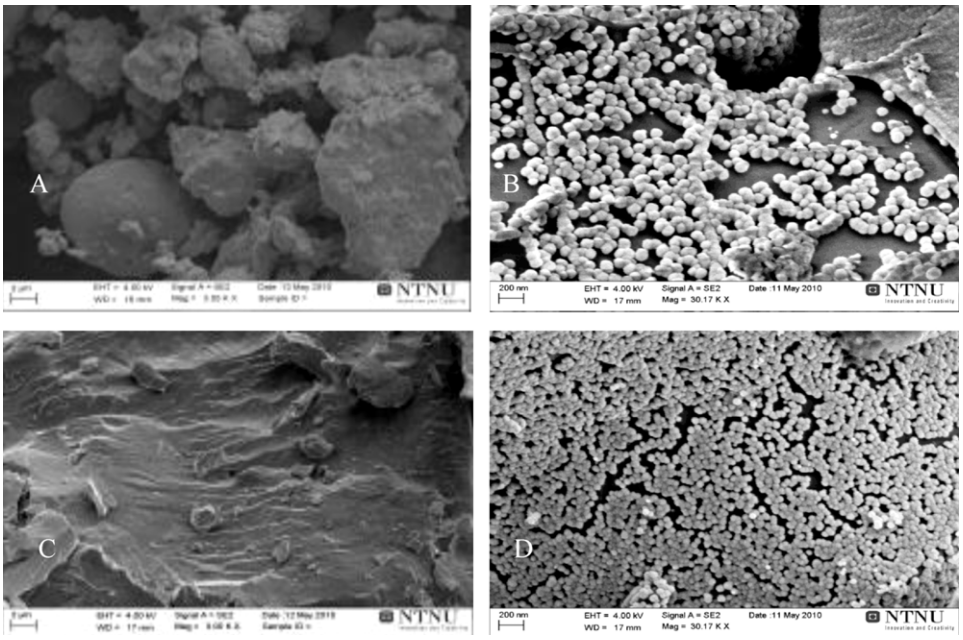

Fig. 2. SEM micrographs for the studies samples. [A] Sintered $Ti_{1.1}Fe_{0.9}O_x$, [B] Sintered $Ti_{1.1}Fe_{0.9}O_x$ after deposition of Pd, [C] Arc–melted TiFe, and [D] Arc–melted TiFe after deposition of Pd.

sponding hydrides[1] were refined using the GSAS software and are shown in Fig. 1.

Both arc-melted and sintered materials contained the bcc-TiFe intermetallic as a major constituent. In addition, the sintered material contained two extra phases including a suboxide η-$Ti_4Fe_2O_{1-x}$ and a solid solution of iron in β-Ti. The hydrogenated samples contain a mixture of β-TiFeH and γ-$TiFeH_2$ intermetallic hydrides, most probably, because of a partial decomposition of unstable at ambient conditions γ-$TiFeH_2$ during the XRD measurements. A significant fraction of a non-hydrogenated TiFe was observed during XRD study of the hydrogenated arc-melted sample. The secondary phases formed in the sintered sample formed two hydrides during the hydrogenation, *viz.* η-$Ti_4Fe_2O_{1-x}H_y$ and TiH. In case of the sintered sample, the formation of the Ti-enriched phases was caused by an excess of Ti, ∼22 at.%, at compared to the stoichiometric equiatomic Ti + Fe mixture. The formation of the oxygen-containing mixed η-oxide originated from capturing trace amounts of oxygen present in the used for the sintering argon gas and adsorbed on the surface of starting metal powders during their exposure to air. From EDS analysis, the amount of oxygen in the sample was appr. 2.9 wt.%. It corresponds to the formation of more than 50 wt.% of the Ti_4Fe_2O suboxide. This value significantly exceeds the corresponding estimations derived from the XRD data (Table 1). Most probably, the EDS data were overestimated and taken for the oxygen-enriched thin subsurface layer (∼1 μm) where the secondary X rays were generated, while the XRD data were collected for the bulk sample.

The surface morphologies of the substrate alloys and surface-modified TiFe-based powders were studied by SEM analysis (Fig. 2).

The substrate powder consisted of particles varying in size, which generally exhibited irregular shape and relatively smooth surfaces. All samples exhibited a little porosity. After the autocatalytic Pd(P) deposition, discontinuous surface layers of the fine Pd–P particles were observed (Fig. 2B and D) with an average particle size of the Pd particles about 70 nm. Atomic absorption spectroscopy was used to determine the total Pd loading and revealed Pd concentration of ∼0.6 wt.%. It was also observed that the Pd(P) layer on the surface of the arc-melted TiFe sample formed a denser packing than the Pd(P) layer on the sintered $Ti_{1.1}Fe_{0.9}O_x$. This observation indicates that significantly lower oxygen content at the surface of the arc-melted sample facilitates improved autocatalytic deposition of Pd.

Studies of the hydrogenation performances of the unmodified and Pd(P) surface-modified samples were conducted after pre-exposure of the sample materials to air, with and without pre-activation by vacuum heating. Without vacuum activation, the

[1] First hydrogen absorption was followed by stabilisation of the hydrogenated samples by their exposing to air at T = 77 K, for 10 min.

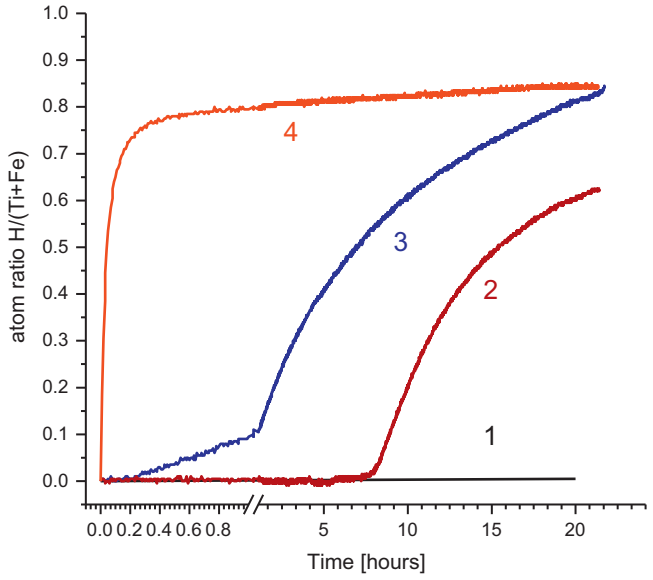

Fig. 3. Hydrogen absorption at $P_0 = 30$ bar and $T = 20\,^{\circ}C$ for the samples of TiFe prepared by arc-melting: 1,3 – unmodified TiFe; 2,4 – TiFe surface-modified by Pd(P) deposition; 1,2 – hydrogenation #1 (no vacuum heating); 3,4 – hydrogenation #2 after vacuum heating to 400 °C for 1 h.

arc-melted (Fig. 3) and sintered (Fig. 4) substrates absorb hydrogen infinitely slowly (curve 1). This is caused by presence of the oxygen-containing layers on the surface, which inhibit transport of atomic hydrogen into the bulk material.

After activation in vacuum by heating at 400 °C, the sintered $Ti_{1.1}Fe_{0.9}O_x$ exhibited better hydrogenation kinetics as compared to the arc-melted TiFe alloy, with an almost eradicated incubation period (compare Figs. 3 and 4; curve 3). The first hydrogen absorption by the sintered material yielded a nearly saturated hydride with H/(Ti + Fe) = 0.9–0.95, as compared to a decreased hydrogen activity of the arc-melted sample, which required several vacuum heating – hydrogen charging cycles to attain maximum absorption

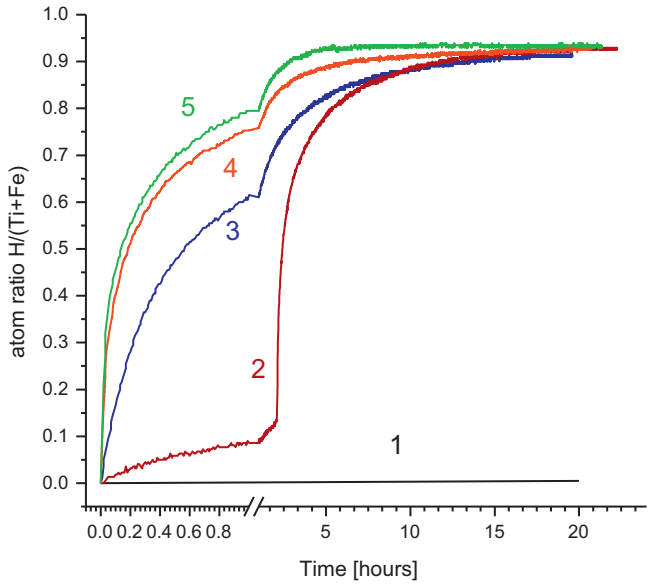

Fig. 4. Hydrogen absorption at $P_0 = 30$ bar and $T = 20\,^{\circ}C$ for samples of $Ti_{1.1}Fe_{0.9}O_x$ prepared by sintering: 1,3 – unmodified substrate; 2,4 – material surface-modified by Pd(P) deposition; 5 – material surface-modified by γ-APTES pre-functionalization followed by Pd(P) deposition; 1,2 – hydrogenation #1 (no vacuum heating); 3–5 – hydrogenation #2 after vacuum heating to 400 °C for 1 h.

capacity. These observations are in compete agreement with the data of the XRD analysis (see Fig. 1c and d for the samples hydrogenated after the first activation). Observed improvement of the hydrogenation activity for the sintered $Ti_{1.1}Fe_{0.9}O_x$ material should be credited to the formation of easy hydrogenated $Ti_4Fe_2O_{1-x}$ and β-Ti acting as hydrogen transfer catalysts, as also observed in [6,20,22].

The improvement of the activation performance of $Ti_{1.15}Fe$ doped by 0.35–0.7 wt.% oxygen (introduced as Fe_2O_3) was also observed by Wakabayashi et al. [12].

The hydrogenation kinetics of the surface-modified materials, carried out without activation by vacuum heating, was significantly faster as compared to that of the unmodified material, albeit with the presence of incubation periods (Fig. 3 and Fig. 4; curve 2). The enhancement can be credited to the partial removal of the surface oxide layers during the chemical treatment, as well as to the enhanced activity of the modified surface towards the H_2 dissociation, due to the presence of the Pd(P) nanoparticles catalyzing H_2 molecule splitting. Similarly to the surface-modified AB_5-type materials [23], it facilitates subsequent diffusion of H atoms into the bulk material and quick attainment of the maximum absorption capacity (curves 2,4).

The sintered $Ti_{1.1}Fe_{0.9}O_x$ functionalized in 1.0 vol.% γ-APTES, and subsequently encapsulated using Pd(P) autocatalytic deposition, exhibited slightly better kinetics of hydrogenation compared to that prepared without the pre-functionalization step (Fig. 4, curve 5). The pre-functionalization step increases the Pd–P density and surface loading thus increasing the surface activity of the materials towards the molecular hydrogen.

4. Conclusions

- This work demonstrates that surface modification of the TiFe-based materials by autocatalytic deposition of Pd(P) results in the formation of discontinuous surface deposits of Pd nanoparticles, causing significant improvement of the activation performances and hydrogen absorption kinetics, despite a long-term exposure of the initial samples to air. The effect was associated with improved catalytic activity of the modified surface towards the H_2 dissociation.
- Sintering of Ti and Fe powder mixtures (1.1:0.9) yielded a formation of $Ti_4Fe_2O_{1-x}$, further to TiFe. The sintered $Ti_{1.1}Fe_{0.9}O_x$ was characterised by a better activation and kinetic performances as compared to the arc-melted TiFe. The effect was associated with the influence of the formed hydrogen transfer catalysts, *viz.* oxygen-containing $Ti_4Fe_2O_{1-x}$ and β-Ti.
- Surface modification of the sintered $Ti_{1.1}Fe_{0.9}O_x$ using a pre-functionalization with water-soluble aminosilane caused improvement of the kinetics of hydrogenation, as compared to the samples prepared by the conventional Pd deposition.

Acknowledgements

This work is supported by Norwegian Research Council and National Research Foundation of South Africa via the Program of Research Co-operation between Norway and South Africa (2007-2010, Project #180344). The activities were carried out within the Hydrogen and Fuel Cell Technologies RDI Programme funded by the Department of Science and Technology in South Africa (project KP3-S02).

References

[1] J.J. Reilly, R.H. Wiswall, Inorg. Chem. 13 (1) (1974) 218–222.
[2] G. Sandrock, J. Alloys Compd. 293–295 (1999) 877–888.
[3] H.H. Van Mall, Patent DE2650276 (1977).

[4] K.N. Semenenko, V.N. Verbetsky, I.L. Varshavsky, E.V. Shatrov, S.V. Mitrokhin, V.S. Zontov, V.V. Gusarov, V.N. Kabalkin, A.Yu. Ramensky, Author's Certificate SU722021 (1981).
[5] Y. Moriwaki, T. Gamou, N. Yanagihara, T. Yamashita, T. Iwaki, Patent US4370163 (1983).
[6] M. Amano, Y. Sasaki, R. Watanabe, M. Shibata, J. Less-Common Met. 89 (1983) 513–518.
[7] A.A. Novakova, O.V. Agladze, B.P. Tarasov, Russ. J. Inorg. Chem. 45 (8) (2000) 1288–1292.
[8] H. Hotta, M. Abe, T. Kuji, H. Uchida, J. Alloys Compd. 439 (2007) 221–226.
[9] M. Abe, T. Kuji, J. Alloys Compd. 446–447 (2007) 200–203.
[10] M.M. Antonova, Yu.G. Privalov, Sov. Powder Metall. and Met. Ceram. 25 (4) (1986) 291–296.
[11] I. Saita, M. Sato, H. Uesugi, T. Akiyama, J. Alloys Compd. 446–447 (2007) 195–199.
[12] R. Wakabayashi, S. Sasaki, T. Akiyama, Int. J. Hydrogen Energy 34 (2009) 5710–5715.
[13] S. Lanyin, L. Fangjie, B. Deyou, Int. J. Hydrogen Energy 15 (4) (1990) 259–262.
[14] J. Ma, H. Pan, X. Wang, C. Chen, Q. Wang, Int. J. Hydrogen Energy 25 (2000) 779–782.
[15] G.D. Sandrock, P.D. Goodell, J. Less-Common Met. 73 (1) (1980) 161–168.
[16] L. Jai-Young, C.N. Park, S.M. Pyun, J. Less-Common Met. 89 (1) (1983) 163–168.
[17] L. Zaluski, A. Zaluska, P. Tessier, J.O. Strom-Olsen, R. Schulz, J. Alloys Compd. 217 (1995) 295–300.
[18] M. Bououdina, D. Fruchart, S. Jacquet, L. Pontonnier, J.L. Soubeyroux, Int. J. Hydrogen Energy 24 (1999) 885–890.
[19] E.M.B. Heller, A.M. Vredenberg, D.O. Boerma, Appl. Surf. Sci. 253 (2006) 771–777.
[20] B. Rupp, J. Less-Common Met. 104 (1984) 51–63.
[21] V.D. Dobrovolsky, S.N. Yendrzheevskaya, A.K. Sinelnichenko, V.V. Skorokhod, O.Yu. Khyzhun, Int. J. Hydrogen Energy 21 (11/12) (1996) 1061–1064.
[22] A.A. Lavrentyev, B.V. Gabrelian, P.N. Shkumat, I.Ya. Nikiforov, I.Yu. Zavaliy, A.K. Sinelnichenko, A.V. Izvekov, O.Yu. Khyzhun, J. Alloys Compd. 492 (2010) 39–43.
[23] M.V. Lototsky, M. Williams, V.A. Yartys, Ye.V. Klochko, V.M. Linkov, J. Alloys Compd. 509 (2011) S555–S561.
[24] G.O Mallory, J.B. Hajdu, Autocatalytic Deposition – Fundam. Appl. 16 (1990) 425–426.
[25] M. Williams, M.V. Lototskyy, A.N. Nechaev, V.M. Linkov, Patent application WO 2009/066263 A1 (ZA 2007/09455).
[26] M. Williams, A.N. Nechaev, M.V. Lototsky, V.A. Yartys, J.K. Solberg, R.V. Denys, C. Pineda, Q. Li, V.M. Linkov, Mat. Chem. Phys. 115 (2009) 136–141.
[27] H.P. Stuwe, Y. Shimomura, Z. Metallkd. 51 (1960) 180–181.
[28] G. Busch, L. Schlapbach, F. Stucki, P. Fischer, A.F. Andresen, Int. J. Hydrogen Energy 4 (1979) 29–39.
[29] P. Fischer, J. Schefer, K. Yvon, L. Schlapbach, T. Riesterer, J. Less-Common Met. 129 (1987) 39–45.
[30] K. Sumiyama, H. Ezawa, Y. Nakamura, Phys. Status Solidi A 93 (1986) 81–86.
[31] H. Numakura, M. Koiwa, Acta Metall. 32 (1984) 1799–1807.